Results in Control and Optimization 15 (2024) 100434

Contents lists available at ScienceDirect

Results in Control and Optimization

journal homepage: www.elsevier.com/locate/rico

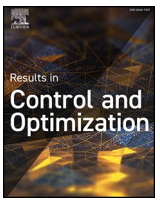

Pneumatic servo position control optimization using adaptive-domain prescribed performance control with evolutionary mating algorithm

Addie Irawan *, Mohd Herwan Sulaiman, Mohd Syakirin Ramli, Mohd Iskandar Putra Azahar

Faculty of Electrical & Electronics Engineering Technology, Universiti Malaysia Pahang Al-Sultan Abdullah, 26600 Pekan, Pahang, Malaysia

ARTICLE INFO

Keywords:
Pneumatic actuator
Prescribed performance control
Evolutionary mating algorithm
Metaheuristic
Data driven

ABSTRACT

Pneumatic servo systems face challenges such as friction, compressibility, and nonlinear dynamics, necessitating advanced control techniques. Research suggests model-based, model-free, hybrid, and optimization-based methods have their strengths. Therefore, this study presents an optimal control strategy using Adaptive Domain Prescribed Performance Control (AD-PPC) cascaded with PID and optimized using the Evolutionary Mating Algorithm (EMA) for a pneumatic servo system (PSS). The goal is to achieve faster transient control and stable rod-piston positioning with minimal friction through the hysteresis phenomenon of the targeted proportional valve-controlled double-acting pneumatic cylinder (PPVDC) representing the PSS. The novel EMA optimizes the cascaded controller based on the tracking error as its objective function. Simulation studies verify the proposed AD-PPC-PID controller with the PPVDC model plant, iteratively optimized by the EMA. The analytical study compares this setup's control system and optimization model with the same control system model using alternative optimization methods. The testing employs step and multi-step signals for PPVDC's rod-piston position input. Results show that the EMA-tuned AD-PPC-PID outperforms AD-PPC-PID controller with other optimizers. For both input trajectory tests, EMA-tuned AD-PPC-PID shows faster response times, with average improvements of 30 % in settling times and 70 % in tracking performance metrics compared to other optimizers, making it robust for nonlinear system applications like PPVDC rod-piston positioning.

Abbreviations: PSS, Pneumatic Servo System; PPVDC, Pneumatic Proportional Valve with a Double-Acting Cylinder; TPG, Tri-Finger Pneumatic Gripper; PID, Proportional Integral and Derivative; DOF, Degree of Freedom; FOPID, Fractional Order PID; PPC, Prescribed Performance Control; PPF, Prescribed Performance Function; AD-PPC, Adaptive Domain Prescribed Performance Control; AC-PPF, Adjustable-Convergence Rate PPF; CPPC, Conventional Prescribed Performance Control; MPC, Model predictive control; ILC, Iterative Learning Control; SMC, Sliding Mode Control; FC, Funnel Control; ADRC, Active Disturbance Rejection Control; ESO, Extended State Observer; PSO, Particle Swarm Optimization; FLC, Fuzzy Logic Control; NN, Neural Networks; LQR, Linear Quadratic Regulator; PAMs, Pneumatic Artificial Muscles; TLBO, Teaching Learning Based Optimization; BMO, Barnacles Mating Optimizer; IAE, Integral Absolute Error; ISE, Integral Square Error; ITAE, Integral Time Absolute Error.

* Corresponding author.
E-mail address: addieirawan@umpsa.edu.my (A. Irawan).

https://doi.org/10.1016/j.rico.2024.100434
Received 28 December 2023; Received in revised form 27 February 2024; Accepted 7 May 2024
Available online 17 May 2024

List of Symbols

M_{rp}	Rod–piston mass
M_L	External payload mass
$A_{i(i=1,2)}$	Absolute pressure in chamber 1 and 2 of the pneumatic cylinder
$\ddot{x}_{rp}$	Acceleration state of the pneumatic cylinder rod–piston
F_f	Inner frictional force in the pneumatic cylinder chamber
F_L	External force of the payload
$u_{dz}(t)$	New control signal with dead-zone characteristic
m_d	Right limits of dead zone
m_e	Left limits of dead zone
z_{md}	Right slopes of the new control signal with deadzone characteristic
z_{me}	Left slopes of the new control signal with deadzone characteristic
$P_{i(i=1,2)}$	Absolute pressures in chamber 1 and chamber 2 of the pneumatic cylinder
t_c	Predetermined convergence of finite-time
$v_{i(i=1,2)}$	Scaling factor
α	Variable-rate convergence function
h	Convergence rate
$\overline{\sigma}$	Upper boundary gain of the PPC
$\underline{\sigma}$	Lower boundary gain of the PPC
$\overline{\sigma}\rho(0)$	Upper limit of the maximum overshoot
$\underline{\sigma}\rho(0)$	Lower limit of the maximum undershoot
$E(t)$	New transformed tracking error
x_d	Reference input of displacement for the rod-piston stroke
$e(t)$	Tracking error
$\Xi(t)$	Normalized error
x_{rp}	Feedback response of displacement for the rod-piston stroke
K_p	Proportional gain of the PID controller
K_i	Integral gain of the PID controller
K_d	Derivative gain of the PID controller
J	Cost function
T	Iteration number
X_m	Solution group for male
X_f	Solution group for female
I_{mates}	Possibility of sexual selection

1. Introduction

Pneumatic systems have become prevalent in industrial and manufacturing settings owing to notable benefits including reliability, favorable power-to-weight ratios, cleanliness, straightforward structural design, cost-effectiveness, and immunity to electromagnetic disturbances. However, complex air flow behavior through valve ports along with the compressibility of air and inherently low natural frequencies introduce accuracy and dynamic performance challenges for pneumatic position/trajectory tracking control. The objective of pneumatic servo system (PSS) control is emphasized not only on the piston positioning but also its pressure stability. Here friction plays a main factor in PSS precisions. Frictional nonlinearities impose difficulties for PSS motion control tasks. The existence of friction in the pneumatic cylinder has both advantages and disadvantages. On the one hand, friction increases damping which can improve system stability. However, friction also causes issues like increased seal wear, lower cylinder output forces, and stick-slip motion at low speeds. Overall, the cons of cylinder friction outweigh the pros. Thus, reducing or eliminating friction has become a major research direction for improving pneumatic cylinder performance. Since most pneumatic cylinders utilize elastic seals, common friction reduction approaches in the pneumatics industry include: enhancing machining precision, utilizing specialized lubricants, designing optimized seal geometries, and employing low-friction materials [1]. However, simply minimizing friction without considering implications on stability can undermine system performance. An integrated approach balancing friction mitigation with stability and control needs may enable optimized pneumatic cylinder designs. When it comes to control issues, identifying the components of uncertainty for the pneumatic servo system that includes its friction is essential. This can be done either through model identification that emphasizes model-based control design strategy or using model-free approaches with various integration methods. The LuGre friction model [2] is the most widely used for modeling and analyzing pneumatic systems, as it captures nonlinear velocity-dependent viscous friction effects. Research [3,4] indicates that lower piston velocities tend to increase static friction, potentially causing jerkier rod movements.

Robust control strategies are therefore vital to address PSS control issues. In the control perspectives, there are various approaches

with various formulations that have been developed to achieve the robustness of the control systems such as model-based, mode-free and hybrid control strategies. Model-based is known for dependent of plant model properties and parameters with the complex control theory [5,6] approaches in its design. Feedforward model compensations [7,8], feedback linearization [9], robust and optimal control [10], and model predictive control [11,12] are the example of model-based controllers that used and implemented by various researchers. Feedforward control employs predictive model plant to determine necessary control inputs for achieving desired motions. For example, in the case of PSS model plant, converting desired outputs into valve duty cycles and compensating for nonlinearities [13, 14]. Alternatively, data-driven models from system identification or neural networks can enhance trajectory tracking accuracy [15, 16]. However, reliance on accurate models has limitations, necessitating the combination of feedforward and feedback mechanisms to ensure robust performance in high-precision applications. Feedback linearization on the other hand, simplifies the plant nonlinearities, facilitating the use of linear control methods and complex numerical solutions [17-19], although unmodeled effects remain. It transforms the plant states for precise control input design, with state estimators aiding unmeasurable state estimation, albeit with computational simplifications [20]. Despite challenges, feedback linearization enhances precision tracking by mitigating nonlinearities [9] for the case of nonlinear model such as PSS. Also, has been used to Model predictive control (MPC) offers slightly different approaches, optimizing inputs by forecasting responses over a finite horizon, minimizing a cost function like tracking error, and systematically handling pneumatic saturation constraints [21]. MPC utilizes prediction horizons to smooth inputs and include coupling constraints. However, computational demands increase with model complexity, necessitating efficient embedded implementation. Overall, MPC provides a promising framework for high-performance for nonlinear plants such as PSS by integrating dynamics models with numerical optimization. Robust control techniques like H-infinity [22] and μ-synthesis [23] as well as super-twisting in adaptive approaches [24,25] enhance stability by directly addressing model uncertainties, while optimal methods such as Linear Quadratic Regulator (LQR) optimize control performance based on analytical models [26], though intensive computations may hinder the limited processor unit such as embedded system implementation.

Model-free control, on the other hand, is the opposite, as it does not require mathematical models of the system dynamics for control law synthesis. Instead, it relies solely on direct input-output data measured from the pneumatic hardware during operation. This provides inherent portability across different plant configurations but critically depends on the availability of high-fidelity sensor feedback measurements. Other than conventional controllers such as PID control, Sliding Mode Control (SMC) [27], Iterative Learning Control (ILC) [28], Prescribed Performance Control (PFC) [29] and Funnel Control [30] are examples of model-free approaches that are majorly deployed with a few adaptive mechanisms in their design. For example, SMC has various adaptive approaches. This control method uses high frequency switching to keep system states on specific surfaces, aiming to drive tracking errors to zero for the targeted plant system. However, achieving accurate tracking depends on precise feedback, while unmodeled effects and hardware limitations, such as imperfect measurements and valve dead bands, challenge its applicability. For instance, Sun et al. proposed integrating SMC with active disturbance rejection control (ADRC) and adaptive control to enhance dynamic response, mitigate chattering, and incorporate an extended state observer (ESO) for improved disturbance rejection. Also, an adaptive law was employed to reduce conservatism in parameter selection [24]. Conversely, ILC aims to enhance tracking accuracy over repeated motions by learning from past errors, adjusting feedforward inputs iteratively for cyclical operations/tasks. Model knowledge isn't necessary since corrections are applied directly through repetition, but stability relies on repeatable dynamics, posing challenges for the plant system under variable conditions. Here, adaptive laws are crucial for ensuring convergence despite varying trial conditions, while advanced robust ILC techniques show potential by combining repetition with real-time compensation for uncertainties. For example, a high-order pseudopartial derivative-based model-free adaptive iterative learning controller was proposed by [31] to enhance tracking control for pneumatic artificial muscles (PAMs), demonstrating improved convergence and tracking performance through theoretical analysis and simulations/experiments. More enhancement works on ILC have been done in [28,32], whereby ILC algorithm was deployed with adaptive elements and cascading approaches to address nonlinearities and uncertainties in PSS, demonstrating its capability to track non-repetitive signals and overcome internal and payload uncertainties.

Another model-free approach that has recently been deployed by various researchers are prescribed performance and funnel control. This type of control approach aims to regulate system behavior within desired bounds. The difference between these two approaches is that prescribed performance control (PPC) focuses on predefined performance objectives, while funnel control (FC whereby the ILC algorithm was deployed with adaptive elements and cascading approaches to address nonlinearities and uncertainties in PSS, demonstrating its capability to track non-repetitive signals and overcome internal and payload uncertainties. Another model-free approach that has recently been deployed by various researchers is prescribed performance and funnel control. This type of control approach aims to regulate system behavior within desired bounds. The difference between these two approaches is that prescribed performance control (PPC) focuses on predefined performance objectives, while funnel control (FC) [33] employs adaptive strategies to guide the system towards desired states. The foundation of PPC was introduced by Bechlioulis et al., where the design was emphasized to ensure system output convergence within strict bounds on overshoot and steady-state error [34]. The FC, on the other hand, was introduced by Ilchmann et al. to cope with all plants of class S, without parameter estimation or identification as well as tolerating noise measurement and huge parameters [35]. For example, Zhang et al. [36] proposed a novel proportional-integral approximation-free control by using PPFs for nonlinear robotic systems without employing any function approximation. To stabilize the vertical and pitch displacements of active suspensions with parametric uncertainties, an adaptive control with PPF constraints was proposed by Jing Na in [37]. For the funnel control implementation, Ueno et al. had proposed this controller design alongside an operator-based nonlinear control system with a boundary function design scheme for pneumatic soft-actuator. This method is to improve their previous works with λ-tracking control that faced excessively large gains over time issues [38]. Moreover, funnel controller deployment has been enhanced a few recent control engineering works such as reported in [39-41] with adaptive elements. For example, Poursadegh et al. had proposed the adaptive finite-time funnel control approach for non-affine strict-feedback nonlinear

systems, handling unknown non-smooth input nonlinearities with FLC and ensuring steady-state and transient performance via improved funnel error surfaces, adaptive laws, and a continuous robust term for enhanced control robustness. Nonetheless, Verginis had utilized zeroing control barrier functions for trajectory tracking within a predefined funnel in control-affine nonlinear systems with unknown drift terms and parametric uncertainties, ensuring bounded control effort and compensating for system uncertainties.

Hybrid control methods blend all mentioned approaches in the control system to maximize the strengths and minimize the limitations of each controller. The fundamental of this approach is based on the cascading and integration technique that involved not only adaptive compensators or coordination between the same controllers but also integration with artificial intelligent algorithms through intelligent control techniques such as fuzzy logic [42,43] and neural networks (NN) [44,45] or computational intelligence to optimize the tuning parameters such as metaheuristic methods [46-50]. In the case of actuator/motor control such as PSS control, as far as we know, the implementation of FLC is more favorable compared to NN when considering the computational factor in real-time operating systems. NN deployment majorly focuses on high computational applications such as image processing [44,51] and vision-based control systems [52,53] in which recently emphasized deep learning approaches. For example, Dhami had implemented a hybrid control approach combining FLC and SMC for effective position control strategy for a pneumatic actuation system by leveraging both techniques to cater to both low and high payload situations [54]. Similarly, in [55] self-tuning was designed using FLC for controller switching to increase the transient response of pneumatic rod-piston positioning and reduce the hysteresis effect. Slightly different from [56] whereby the state observer for PSS was constructed by the FLC considering input voltage saturation and full-state constraints, ensuring control performance and guaranteeing bounded signals and adherence to constraints. Dai et al. on the other hand proposed a hybrid MPC and ILC method to enable real-time dynamic modeling and precise trajectory tracking for pneumatic soft robots. Here, the proposed method performed both model parameter learning and trajectory tracking control for the targeted PSS [57].

Complex and nonlinear dynamics inherent in practical engineering systems such as pneumatic actuators and controls pose obstacles for effective management, especially in providing fine-tuning for optimal performance. Addressing these challenges involves leveraging optimization strategies coupled with computational intelligence disciplines, showcasing growing utility in improving control system performance. Notably, techniques based on function approximation play a crucial role in managing unmodeled nonlinearities and uncertainties. Simultaneously, metaheuristic machine learning approaches serve as essential tools for navigating intricate design spaces efficiently, leading to the acquisition of high-quality solutions. These methodologies exhibit valuable generalization capabilities and play a central role in optimizing parameters for effective control tasks. Various metaheuristic categories exist spanning decades of research: Evolutionary Algorithms (EA), Physics-Based Algorithms (PBA), Human-Based Algorithms (HBA) and Swarm Intelligence (SI). EAs are drawn from biological evolution principles to produce next-generation solutions via inheritance from parents. A prominent EA class member, Genetic Algorithms (GA) [58], has successfully solved optimization problems across fields including forecasting [59], marketing/economics [60], communication systems, numerical and statistical analysis [61] as well as engineering solutions [62]. For instance, in the robotics field, GAs were used for optimizing self-learning dynamic walking parameters for a quadrupedal robot to improve its walking stability by emphasizing its active back part as reported in [63]. GAs have also been deployed in time series analysis and second-order boundary value problems in numerical domains such as reported in [61,64,65].

Other EAs include Differential Evolution (DE) [66] and Evolutionary Programming [67]. SI methodologies mimic social group behavior; Particle Swarm Optimization (PSO) [68] emulates bird flocking patterns, while Ant Colony Optimization (ACO) [69] was inspired by ant colony behavior. PSO is a popular SI method used in various fields, especially control engineering [70,71] and image processing [72], due to its rapid convergence and ease of implementation. More SI methods draw inspiration from natural behavior such as Artificial Bee Colony (ABC) algorithm [73] from bees, Grey Wolf Optimizer (GWO) [74] from wolf-packs, Moth Flame Optimizer (MFO) from moths, Crow Search Algorithm (CSA) [75] from crows, and Barnacles Mating Optimizer (BMO) [76] from barnacle's mating process. Additionally, Gravitational Search Algorithm (GSA) [77], motivated by Newton's gravity law, exemplifies PBA. Alternatively, the Human-Based Harmony Search Algorithm (HSA) [78] arose from musical improvisation principles. Both GSA and HSA have proven effective optimization across myriad application domains.

For optimizing hybrid or cascaded controller structures with multiple tunable parameters, selection or design of an efficient and practical optimizer is essential. The optimizer plays a key role in revealing the actual potential and robustness of the control system design and demonstrates practicality in terms of computational cost. For instance, Parnichkun and Tuvayanond selected PSO to optimize their proposed 2-DOF H∞ loop shaping controller for a 3-DOF pneumatic surgical robot, covering closed-loop dynamics, robustness, and minimal control input compared to conventional methods, proving effectiveness for Minimally Invasive Surgery (MIS) [79]. Alternatively, Leader-based Harris Hawks Optimization (LHHO) was deployed in [80] for cascaded PID and Fractional Order PID (FOPID) controller design to effectively regulate DC motor speed. For HVAC systems, Jin and Wang proposed online optimization using GA on multiple tuning parameters in variable air volume (VAV) systems to achieve self-tuning behavior [81]. In [82], GAs again optimized a proposed hybrid PID-LQR controller with prescribed stability for Rubber Tyred Gantry Cranes. A new bi-level cross entropy algorithm was proposed in [83] to optimize aircraft arrival sequences, aiming to minimize combined fuel consumption while each aircraft follows an optimal trajectory. It combines cross-entropy for combinatorial sequencing and direct collocation for optimal control, validated through a test case and demonstrating superior performance compared to a bi-level GA. As for summary, in many successful approaches discussed earlier there are still a gap in guidance and selecting the most efficient and practical optimization algorithm for tuning parameters in hybrid and cascaded control systems. Different applications and controller structures may benefit from different optimizers. Practical considerations like computational cost must be balanced with optimization performance. There is no one-size-fits-all best approach.

To address the challenging issues of nonlinearity and uncertainty inherent in PSS tracking error, this paper presents an Adaptive Domain Prescribed Performance Control (AD-PPC) strategy paired with a Proportional-Integral-Derivative (PID) controller, optimized using a novel Evolutionary Mating Algorithm (EMA) [84]. The control approach is verified on a proportional valve-controlled

double-acting pneumatic cylinder (PPVDC) model plant, which represents PSS nonlinear dynamics. The main contributions are summarized as follows:

1. An adaptive PPC method enables finite-time transient control and convergence rate specifications, along with sufficient error transformation boundary domains. This overcomes limitations of conventional PPC (CPPC) [34], which constrain control engineering implementations. The design focuses not only on increasing the speed of transient response but also on the overall stability of the PSS.
2. EMA-based iterative tuning of the cascaded AD-PPC-PID controller was conducted through simulations using a PPVDC system model. This demonstrates a data-driven optimization approach for the control parameters to accommodate time-variant (simulation-time) data from the plant model with injected random noise.

The rest of the paper is organized as follows: Section II details the PPVDC system dynamics, AD-PPC formulation and integration with PID control. Section III presents EMA implementation for optimizing AD-PPC-PID controller parameters to regulate PPVDC rod-piston positioning. Section IV analyzes and verifies EMA-tuned AD-PPC-PID controller performance under step and multi-step reference trajectories, comparing it against results from other optimizers using the same controller structure. Finally, Section V summarizes pneumatic positioning system performance enhancements enabled by the control approach.

2. Controller design

As mentioned earlier, this study focused on the PPVDC dynamic model that represented the physical PPVDC attached to the Tri-pneumatic Grasper (TPG) [85] robot as shown in Fig. 1. The general overview of the model plant can be explained by the following motion equation governing the piston and kinematics response [55,86];

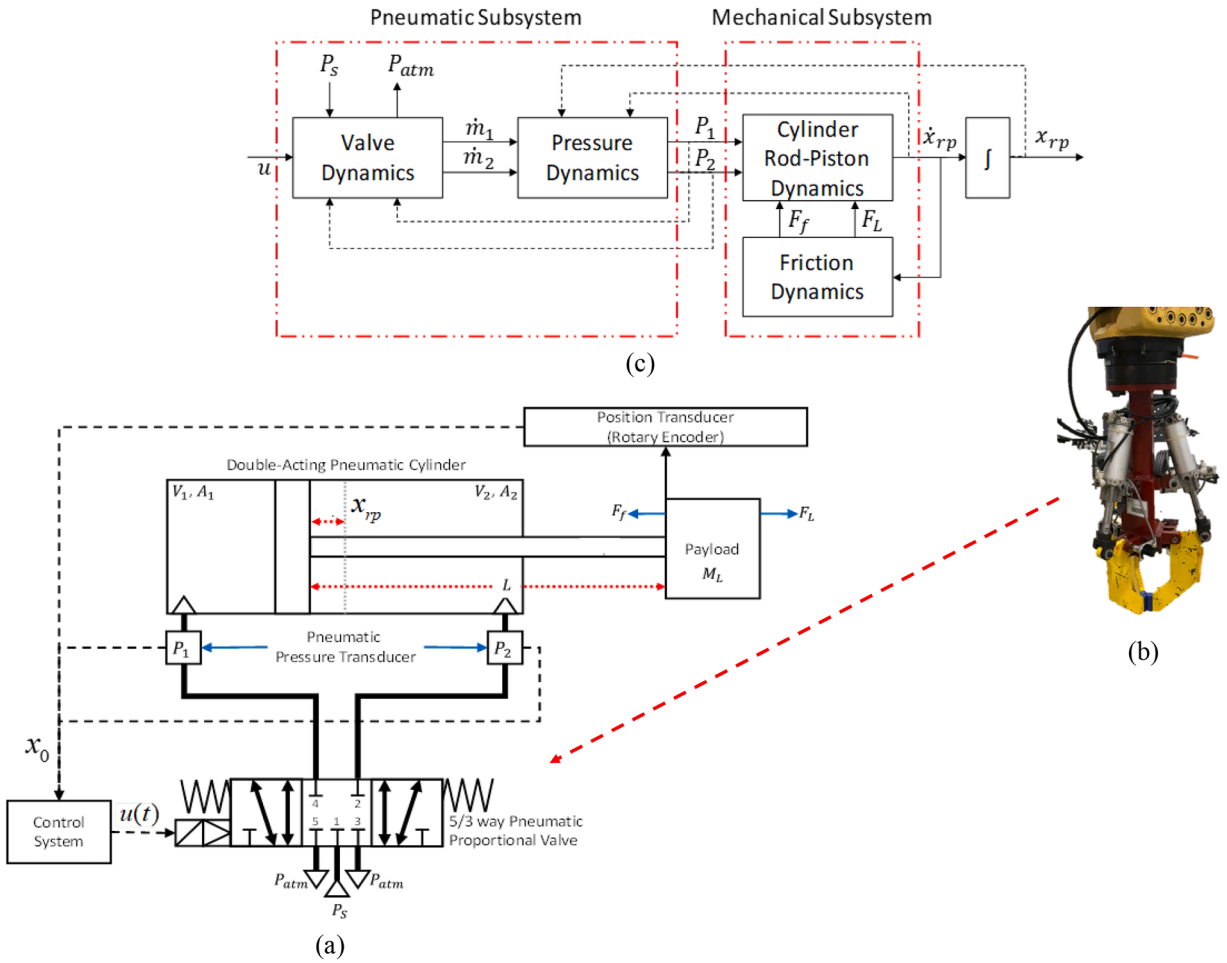

Fig. 1. Overview of PPVDC system structure; (a) schematic diagram, (b) attached application (TPG robot), and (c) mathematical model [86].

$$\ddot{x}_{rp} = \frac{A_1 P_1 - A_2 P_2 - (F_f - F_L)}{M_p + M_L} \tag{1}$$

Here, external payload mass and the rod-piston mass are represented by M_L and M_{rp}, respectively. The annulus regions of each of the pneumatic cylinder rod-piston chambers are denoted by $A_{i(i=1,2)}$. Meanwhile, P_1 and P_2 represent the absolute pressures in Chamber 1 and Chamber 2 of the pneumatic cylinder, respectively. $\ddot{x}_{rp}$ denotes the acceleration state of the pneumatic cylinder rod-piston assembly. Additionally, F_f and F_L refer to the inner frictional force inside the pneumatic cylinder chamber and the external force exerted by the payload, respectively, as illustrated in Fig. 1(a). Conversely, the input of the plant is expressed with the deadzone characteristics,$u_{dz}(t)$,as follows [55];

$$u_{dz}(t) = \begin{cases} m_d[u(t) - z_{md}] & ,if \quad u(t) \geq z_{md} \\ 0 & ,if \quad z_{me}u(t) < z_{md} \\ m_e[u(t) - z_{me}] & ,if \quad u(t) \leq z_{me} \end{cases} \tag{2}$$

where z_{md} and z_{me} are the right and left slopes of $u_{dz}(t)$. Both m_d and m_e are the right and left limitations of the deadzone, respectively. The overall PPVDC dynamic model, based on the LuGre friction model [2], is shown in Fig. 1(c) and detail on this model can be found in the previous studies reported in [55,86]. The tracking error for positioning is referred to the different between the input trajectory (x_{rp}) and the feedback response of the rod-piston position (x_0) as follows;

$$e = x_{rp} - x_o \tag{3}$$

2.1. Adaptive domain prescribed performance function

In this study the conjunction or cascaded method has been approached to improve the performance of PPVDC's rod-piston positioning. The previous variable-rate convergence and finite-time prescribed performance function (VRC-PPF) [87] is improved and the revision has been made on the domain boundary function, $\left[\overline{\sigma}, \underline{\sigma}\right]$. According to the smooth function of VRC prescribed performance function (PPF) as follows:

$$\rho(t) = (\rho_0 - \rho_\infty)e^{-ht} + \rho_\infty \tag{4}$$

where

$$h = \frac{2\alpha^2}{t_c^2} \tag{5}$$

and

$$\alpha = v_1 t(\tanh[v_2(t - t_c)] + 1) \tag{6}$$

t_c is the predetermined convergence of finite-time [88], and both v_1 and v_2 are positive finite scaling factor for finite time and converge-rate respectively, with default value of 1 in the variable-rate convergence function (α). On the other hand,$\rho_0$represents the initial value of the tracking error at the transient, while the maximum permissible range of the error boundary (ρ_∞) is reached at $\rho_0 > \rho_\infty > 0$. As per the original formula of PPC [34], the concrete convergence time cannot be prescribed by the user when $\lim_{t\to\infty}\rho(t) = \rho(\infty) > 0$with $\rho(t)$ is positively decreasing and $t \equiv \infty$ as reaches the stability boundary($\rho(\infty)$). Therefore, the new $\left[\overline{\sigma}, \underline{\sigma}\right]$ can be formulated as a new adaptive domain (σ_c) by proportional with the dynamically changed with of h makes $\overline{\sigma}_c \neq \underline{\sigma}_c$ as follows;

$$\begin{aligned} \overline{\sigma}_c &= (\overline{\sigma} - 1)h + 1 \\ \underline{\sigma}_c &= \left(\underline{\sigma} - 1\right)h + 1 \end{aligned} \tag{7}$$

with the condition.

$$\begin{aligned} &\lim_{t\to\infty}\overline{\sigma}_c > 1, \ \ \overline{\sigma} \geq 1 \\ &\lim_{t\to\infty}\underline{\sigma}_c > 1, \ \ \underline{\sigma} \geq 1 \end{aligned} \tag{8}$$

where the steady-state-error performance ($e(t)$) can be achieved with the defined performance function as follows;

$$-\underline{\sigma}_c\rho(t) < e(t) < \overline{\sigma}_c\rho(t), \forall t > 0 \tag{9}$$

2.2. Error transformation

In prescribing process of the PPC, an error transformation was introduced for converting the constrained objective function, represented by $e(t)$ into an unconstrained formulation that highlights the relationship between$\rho(t)$from (4) and $e(t)$ as follows;

$$e(t) = \rho(t)S(\mathrm{E}) \tag{10}$$

where,

$$S(\mathrm{E}(t)) = \frac{\overline{\sigma}_c e^{\varepsilon(t)} - \underline{\sigma}_c e^{-\varepsilon(t)}}{e^{\varepsilon(t)} + e^{-\varepsilon(t)}} \tag{11}$$

and $\mathrm{E}(t)$ is a new transformed error and developed to the increase function $S(\mathrm{E})$. The $|e(t)| < \rho(t), \forall t \geq 0$is obtain since the function of $S(\mathrm{E})$ is strictly monotonic increasing. On the other hand, defining $\rho(t)$can be done to control the behavior for both transient response as well as the steady error input of the closed-loop controller. The inverse transformation function for the bounded $\mathrm{E}(t)$can be described as follows:

$$\mathrm{E}(t) = S^{-1}\left(\frac{e(t)}{\rho(t)}\right) = \frac{1}{2}\ln\left(\frac{\Xi(t)+1}{1-\Xi(t)}\right) \tag{12}$$

where $S^{-1}(\bullet)$ is the inverse function of $S(\varepsilon)$ and normalized error $\Xi(t) = e(t)/\rho(t)$ at $|\mathrm{E}(0)| < 1$. Moreover, $\Xi(t)$ satisfies $-1 < \Xi(t) < 1$whenever $\mathrm{E}(t) \neq \infty$and the predefined bound of PPF [88] is guaranteed whenever $\mathrm{E}(t)$ is constantly bounded. The control objective is analogous to creating the positioning control in such a way that $\mathrm{E}(t)$ is constrained. Thus, the PID controller's control input for PPVDC's rod-piston positioning with AD-PPC can be stated as follows:

$$u(t) = K_p\mathrm{E}(t) + K_i\int \mathrm{E}(t)dt + K_d\frac{d}{dt}\mathrm{E}(t) \tag{13}$$

where K_p, K_i and $K_d$are the positive finite design parameters for PID controller.

3. Controller optimization using evolutionary mating algorithm

As stated previously, to concurrently optimize the parameters of both the decay function in PPF $\{\rho_o, t_c, \rho_\infty, \nu_2\}$ and the PID parameters $\{K_p, K_i, K_d\}$, an EMA [84] is utilized as depicted in Fig. 3. The ν_1 parameter is preset to 1 for this system design since prior work [88] identified this as the optimal value. The state feedback control law for the AD-PPC-PID can be represented as a single entity. Overall, the state feedback control law for the AD-PPC-PID controller can be expressed compactly in the form of $\Gamma := \begin{bmatrix} K_p & K_i & K_d & \rho_o & t_c & \rho_\infty & \nu_2 \end{bmatrix}^T \in \mathscr{R}^7$.

Problem 1: The optimal solution $\Gamma^* \in \mathscr{R}^7$such that

$$\Gamma^* := \arg\min_{\Gamma} J(\Gamma). \tag{14}$$

where the cost function (J) quantifies the total simulation runtime(t), per iteration (k) to be minimized by the optimization, which is expressed;

$$J(\Gamma, k) := |\mathrm{E}(t)|. \tag{15}$$

where the maximum number of iterations is denoted by $T_{max} \in \mathscr{R}$, while the current iteration number is given by T. Similar to various other metaheuristic algorithms, the EMA commences with an initialization phase, proceeds to a selection phase, and culminates in the generation of new offspring.

3.1. Initialization

In this stage, the solution (X) is initiated in two groups; males (X_m) and females (X_f). The composition of these groups can be defined as follows:

$$X_m = \begin{bmatrix} x_1^1 & \cdots & x_1^d \\ \vdots & \ddots & \vdots \\ x_{n/2}^1 & \cdots & x_{n/2}^d \end{bmatrix} \tag{16}$$

$$X_m = \begin{bmatrix} x_{\frac{n}{2}}^1 + 1 & \cdots & x_{\frac{n}{2}}^d + 1 \\ \vdots & \ddots & \vdots \\ x_{\frac{n}{2}}^1 + 1 & \cdots & x_{\frac{n}{2}}^d + 1 \end{bmatrix} \tag{17}$$

where d and n are denoted by problem dimension and population size, respectively. Following the initialization phase, the objective or fitness function is computed for each individual within the population. Subsequently, the best solution up to the current point is

determined, considering both X_m and X_f, and is then recorded for further reference. This process ensures ongoing evaluation and tracking of the most promising solutions throughout the algorithmic progression.

3.2. Process of selection for mating

The mating process in EMA is facilitated by the possibility of sexual selection, referred to as I_{mates}, which is outlined in a more straightforward manner [20], as follows:

$$I_{mates} = 1 + \left[\text{var}\left(X_m^T, *\right) - \text{var}\left(X_f^T, *\right)\right] \tag{18}$$

where $var(X_m, {}^T_*)$ and $var(X_f^T{}_*)$ are the variance of the selected male and female to be mated, respectively at iteration T.

3.3. Off springs reproduction process

The productions of new off springs, X_{child}^T, are calculated using the following expression:

$$X_{child}^T = \begin{cases} p. * X_{m,*}^T + q. * x_{f,*}^T & I_{mates} \geq 0 \\ p. * X_{f,*}^T + q. * x_{m,*}^T & I_{mates} < 0 \end{cases} \tag{19}$$

where p is the normal random distribution, which is expressed as follow:

$$p = randn(1, d) \tag{20}$$

where q = 1- p. Suppose that at the last iteration, the optimum location of the agent, $p^* \in \mathscr{R}^{1\times d}$, is found, such that it yields the minimum value of the fitness function. In that case, all agents are expected to converge to this location, implying that:

$$p^* := \underset{p_n}{\text{arg}min} f_{fit}, \forall n. \tag{21}$$

where $f_{fit} = J$. EMA incorporates the influence of environmental factors, specifically the predator-prey scenario, considered as an exploratory process. This results in a significant alteration of the optimal solution's characteristics, contingent upon whether the

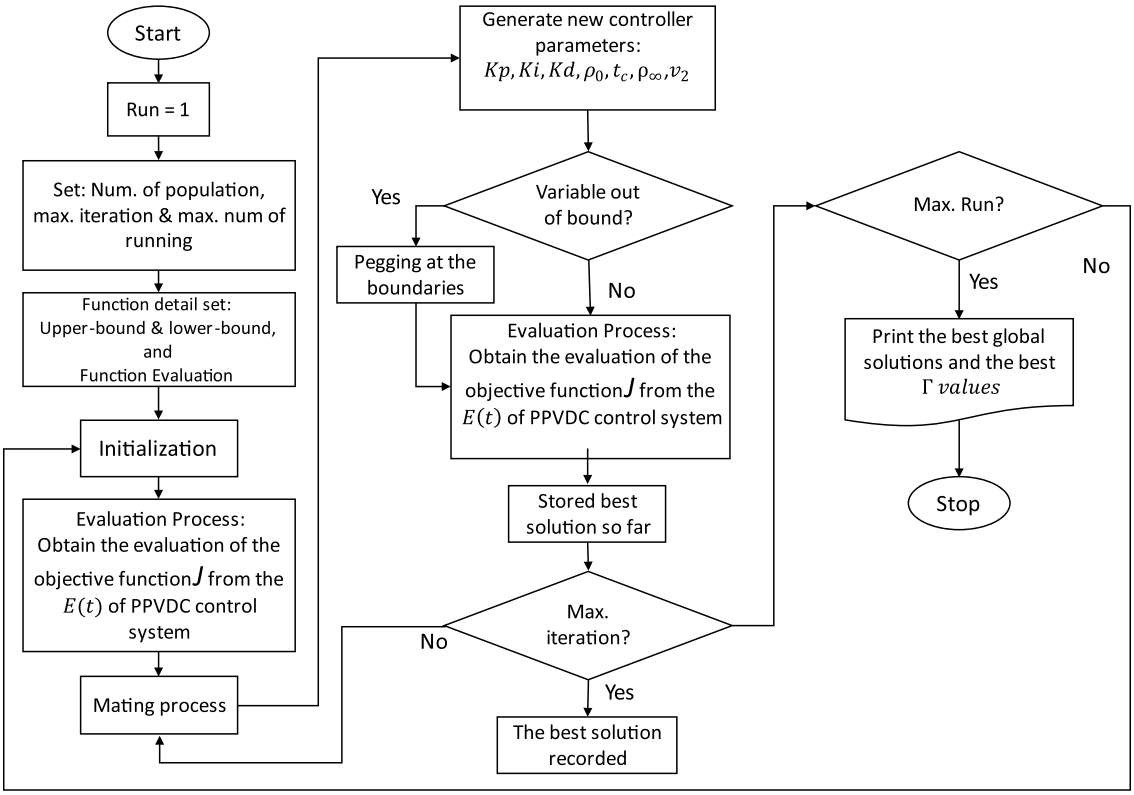

Fig. 2. Overall deployment of EMA algorithm for AD-PPC-PID controller parameters tuning for PPVDC rod-piston positioning.

offspring is presumed to be deceased or alive. More comprehensive details on EMA can be found in [20], and Fig. 2 visually presents the overall deployment of EMA in AD-PPC-PID tuning in detail.

Additionally, Fig. 3 provides a functional block diagram of the overall control system design for PPVDC rod-piston position control, highlighting the utilization of the AD-PPC-PID controller with EMA serving as the optimizer.

4. Results and discussions

Simulation studies were conducted to verify the proposed AD-PPC-PID with EMA optimization control strategy by comparing it with the same controller that optimized using existed metaheuristic methods which are genetic algorithm (GA) [89], Teaching Learning Based Optimization (TLBO) [90] and Barnacles Mating Optimizer (BMO) [76] on the identical PPVDC plant. This verification works underwent one basic input trajectory which is step input and one crucial input trajectory multi-step inputs for rod-piston positioning of PPVDC. This work is done and setup using the MATLAB®/SIMULINK environment and using the data driven concept by testing the proposed controller with the targeted plant and direct collecting the data for each iteration. An external disturbance in the form of random noises was added to the system at around 1–2 kHz according to the current existed hardware system [91]. Overall simulation was set to 10 s for each iteration. The simulation was started with a step input trajectory as fundamental test to the proposed AD-PPC-PID on PPVDC rod-piston positioning. The analysis was carried out to observe and confirm the precision of PPVDC rod-piston positioning, as well as the stability of the internal pneumatic cylinder, with the convergence of EMA and other optimizers with the AD-PPC-PID controller.

4.1. Step input trajectory test

The simulation involved setting the step input of the PPVDC's rod-piston to a length of 0–0.1 m. Tables 1 displayed the optimal results obtained by using EMA and other optimizers to PPVDC's rod-piston positioning according to the step input given. All optimizers showed success in obtaining the parameters within the specified range, which is represented by the optimizer boundaries of Min. (lower bound) and Max. (upper bound). The specified range is determined according to the experiences and hardware constraint from the previous studies [43,88,92,93].

The robustness of each optimizer-controller combination was evaluated based on three measures: rise time, settling time, and overshoot including the different pressures and the constraint boundary or smooth function performances of the PPF. From this point onward in the discussion, the AD-PPC-PID controller tuned with EMA, represented by 'EMA' in the plot, and the AD-PPC-PID controller with other optimizers are denoted as optimizer shortforms 'GA', 'TLBO', and 'BMO' in the plot, respectively. As shown in Fig. 4, the EMA yielded superior controller tuning performance relative to the benchmark optimization methods for the AD-PPC-PID controller. EMA produced transient responses with reduced rise times between 0.3 to 0.6 s based on the position displacement profile of the piston-rod apparatus. The majority of optimizer tuning schemes elicited minimal oscillatory behaviors without considerable overshoot. However, the tuning mechanism mediated by EMA reduced settling times by an average of 0.5 s compared to AD-PPC-PID controller tuned by other optimizers. This enhancement may be attributed to the smooth objective function landscape navigated by EMA in Fig. 5. Specifically, EMA defined an optimal control parameter boundary in approximately half the function evaluations as AD-PPC-PID controller tuned by the GA and reached the terminal control configuration ahead of the remaining optimizers in terms of finite convergence time.

Regarding computational factors, as depicted in Fig. 6, EMA surpassed all other optimizers in minimizing error, indicated by the cost function (J). As shown in Fig. 6(a), EMA reduced $J$from 0.015 % at the first function evaluation $k = 1$ down to $J = 0.0012\%$ by the $k = 10$, while the GA only decreased J from 0.016 % to 0.014 % across the same iterations. On average, EMA achieved a cost function value 10 % lower than GA, 20 % lower than TLBO, and 43 % lower than BMO at convergence. Additionally, EMA exhibited the lowest

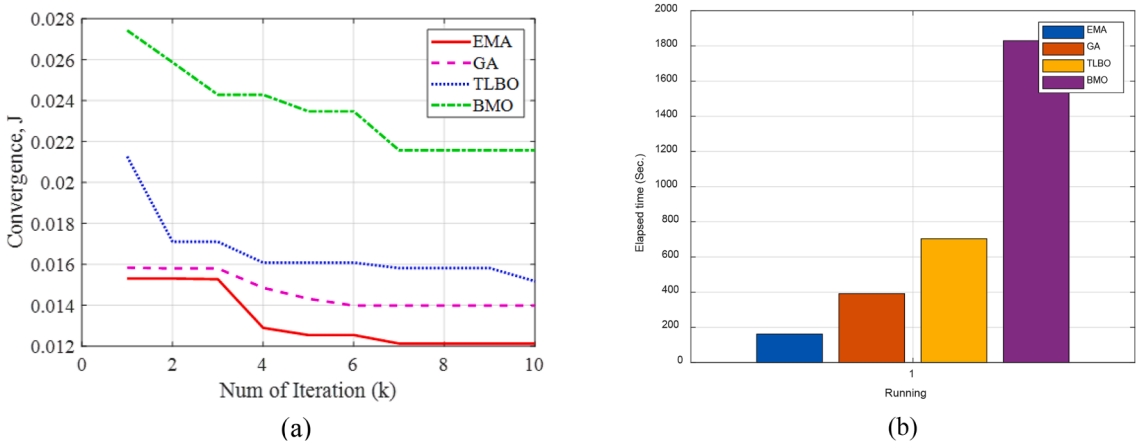

Fig. 3. Overall control structure of EMA with AD-PPC-PID controller for PPVDC rod-piston positioning.

Table 1
FT-PPC-PID controller parameters for step input trajectory test.

Controller / Optimizer	PID			AD-PPC			
	P	I	D	ρ_0	t_c	ρ_∞	ν_2
Min. (lower bound)	20	2	5	5	0.5	1	1
Max. (upper bound)	60	8	7	15	1.2	5	5
EMA	23.9949	3.5080	0.8167	5.7225	0.1800	1.7996	1.7916
GA	51.8180	1.9838	4.9664	12.5201	0.6267	3.8895	1.7183
TLBO	39.7595	7.1637	6.0121	10.2077	0.6559	1.0017	1.8968
BMO	38.6831	6.5516	5.4405	12.3937	0.5187	1.0204	1.8165

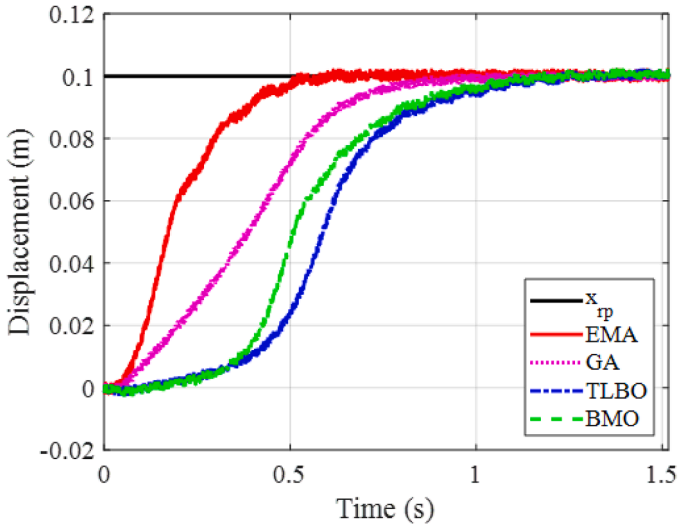

Fig. 4. Sample of rod-piston displacement performances between AD-PPC-PID with optimizers for step input trajectory.

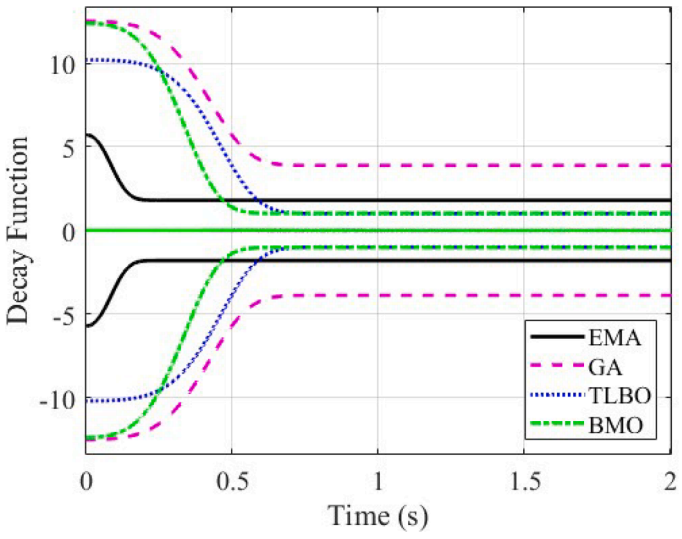

Fig. 5. Sample of decay smooth function performances between AD-PPC-PID with EMA and AD-PPC-PID with other optimizers for step input trajectory.

computational cost among other heuristic methods, as shown in Fig. 6(b), in tuning AD-PPC-PID controller for PPVDC's rod-piston positioning. BMO consumed a significantly higher amount of elapsed time, approximately 90 % more than EMA.

In terms of time response and robustness performance, as shown in Table 2, tuning the AD-PPC-PID using EMA (represented by

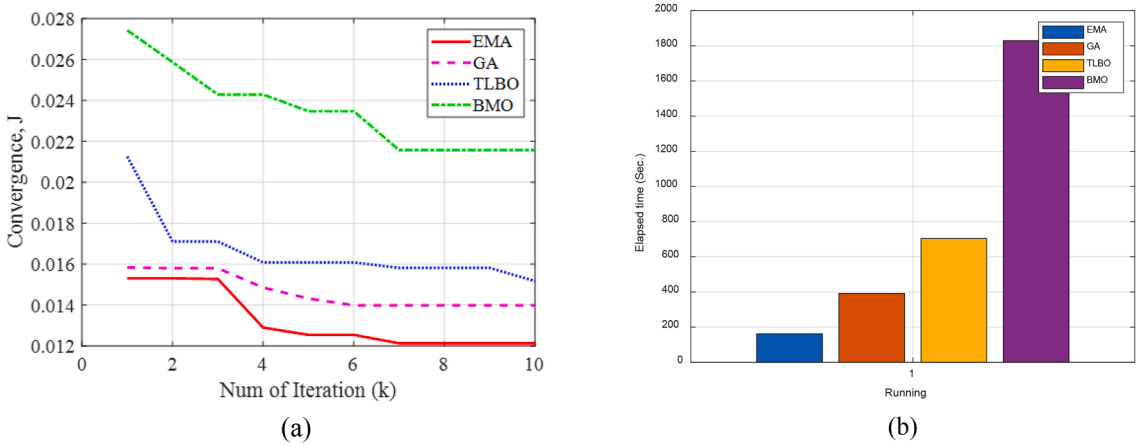

Fig. 6. Sample of computational cost between optimizers used in tuning AD-PPC-PID controller, (a) convergence (b) Elapsed time of simulation.

Table 2
Performance and robustness of the controllers for step input trajectory test.

Performance	AD-PPC-PID Controller with			
	EMA	GA	TLBO	BMO
Rise Time	0.2937s	0.4958s	0.4498s	0.4382s
Settling Time	0.4783s	0.7771s	1.0222s	1.0111s
Transient Time	0.4782s	0.7652s	1.0221s	1.0111s
Overshoot	2.3 %	2.6 %	3.7 %	3.7 %

EMA in the plot) resulted in the fastest responses compared to AD-PPC-PID controller tuned by the other optimization algorithms. This is evident in the rising, settling and transient time results, where EMA outperformed GA by 0.3 s and both TLBO and BMO by 0.6 s. The overshoot performance seems to be affected by noise, as the percentage is very low on average for all approaches. However, AD-PPC-PID controller tuned with EMA exhibits the lowest overshoot among the various tuning methods.

The results were further substantiated by evaluating performance indices using integral absolute error (IAE), integral square error (ISE), and integral time absolute error (ITAE) for a step input trajectory, as shown in Fig. 7. The findings indicate that the AD-PPC-PID controller optimized with EMA exhibits the lowest values, achieving up to 70 % improvement in IAE, ISE, and ITAE compared to the AD-PPC-PID controller optimized with GA, TLBO, and BMO. Specifically, the controller with GA optimization closely follows the performance of the EMA-optimized controller in terms of ISE, with metric values slightly higher by about 30 %. However, TLBO and BMO exhibit significantly higher values for both ITAE and ISE, as depicted in Fig. 7. Interestingly, these optimizers perform similarly lower in IAE compared to GA, achieving approximately 50 % improvement. Overall, these findings suggest that the proposed AD-PPC-PID controller optimized with EMA consistently provides high tracking performance for nonlinear systems, such as PPVDC.

4.2. Multi-step input trajectory test

The verification work was advanced through a multi-step input trajectory test. The test aimed to observe the optimized tuning values for the AD-PPC-PID controller listed in Table 1, catering to multi-step input trajectories to mimic actual situations in PSS applications that currently attached on TPG robot. The evaluation focuses on tracking errors as well as the internal stability of the PPVDC in rod-piston positioning. As depicted in Fig. 8, AD-PPC-PID controller tuned with EMA, on average, has sustained its performance in providing the fastest and most stable responses compared to AD-PPC-PID controller with other optimizers. This can be clearly seen in the tracking error performances in Fig. 8(b), which are about 10 % lower than AD-PPC-PID controller tuned with GA and 60 % to 80 % lower than AD-PPC-PID controller tuned with TLBO and BMO.

The verification and analysis are furthered on the dynamic stability performance of the PPVDC as shown in Figs. 9 and 10. The oscillation in the inner pressures for pneumatic cylinders seems difficult to suppress by using AD-PPC-PID controller tuned with GA and BMO compared to tuning with the EMA and TLBO optimizers. As shown in Fig. 9, PPVDC rod-piston positioning with AD-PPC-PID and EMA control strategies shows oscillating about 0.5–0.6 MPa higher than AD-PPC-PID controller with TLBO at every changed of the step input. However, for the case of using AD-PPC-PID controller with EMA optimizer, the results show that attenuation of the oscillation envelope signal was suppressed over the time in each step input as early as 0.2 s on average compared to AD-PPC-PID controller performances with other optimizers. As depicted in Fig. 9, AD-PPC-PID with GA and BMO also provides oscillation suppression on every step input trajectory but only by minimizing the amplitude and 0.3–0.4 s later than AD-PPC-PID controller tuned with EMA.

The hysteresis effects also differ across control strategies as observable in the friction-velocity characteristics as shown in Fig. 10.

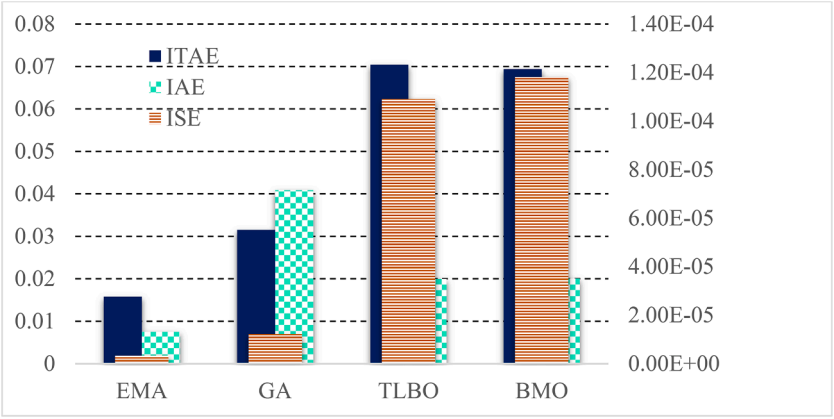

Fig. 7. Performance index.

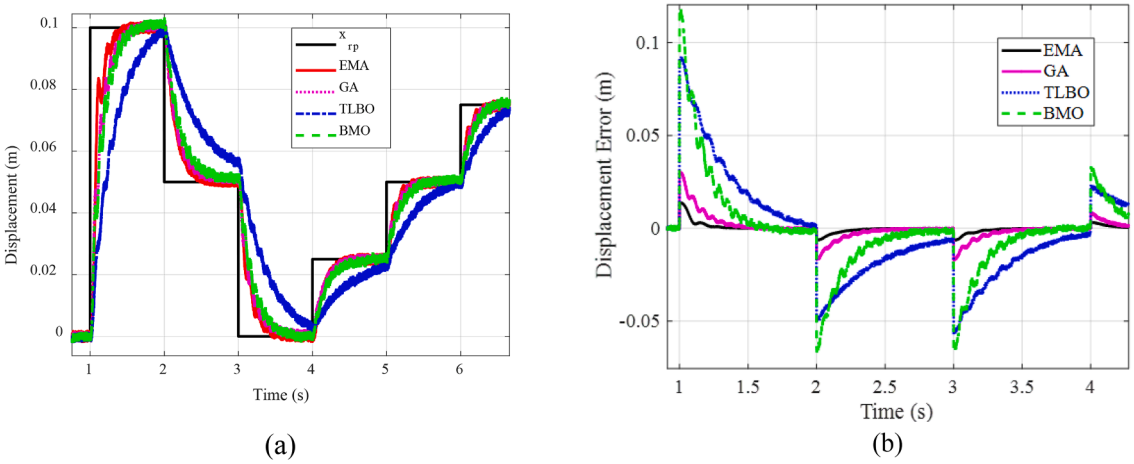

Fig. 8. Sample of rod-piston displacement performances between AD-PPC-PID with EMA and AD-PPC-PID with other optimizers; (a) Input reference versus feedback measured samples (b) Error tracking samples.

The EMA-tuned AD-PPC-PID exhibits minimal narrow hysteresis banding around the zero relative velocity point per the pre-sliding motion curve [94] compared to the other optimizers. Unmitigated oscillations can be transformed into a high mechanical vibration that leads to a high energy valve switching which reduces the life of the pneumatic valve as well as the pneumatic actuator.

5. Conclusion

The proposed AD-PPC-PID control strategy, optimized with EMA, is introduced. This approach is verified using a PPVDC dynamic model plant, employing both step and multi-step input trajectories. The newly devised AD-PPC-PID controller facilitates adaptive domain resizing and adjusting the convergence rate parameters. This offers enhanced finite-time control capabilities of PPC compared to conventional fixed-domain method. Implementation showcases improved transient response and stability in rod-piston positioning across the range of multi-step inputs. The EMA-tuned AD-PPC-PID also diminishes oscillation amplitudes, leading to enhanced steady-state positioning. Notably, minimal pressure oscillations and reduced hysteresis effects indicate that the AD-PPC-PID controller, tuned with EMA optimizers, effectively addresses pressure stability issues inherent in PSS such PPVDC unit, including friction problems. These findings affirm the robustness of the AD-PPC-PID tuned with EMA optimizer for PSS applications such as PPVDC units, in terms of precision and stability control. Ongoing efforts aim to implement the optimized AD-PPC-PID control on the actual TPG robot system, accounting for real hardware constraints. This may entail further modifications to the controller and fine-tuning to optimize performance.

Declaration of competing interest

The authors declare that they have no known competing financial interests or personal relationships that could have appeared to

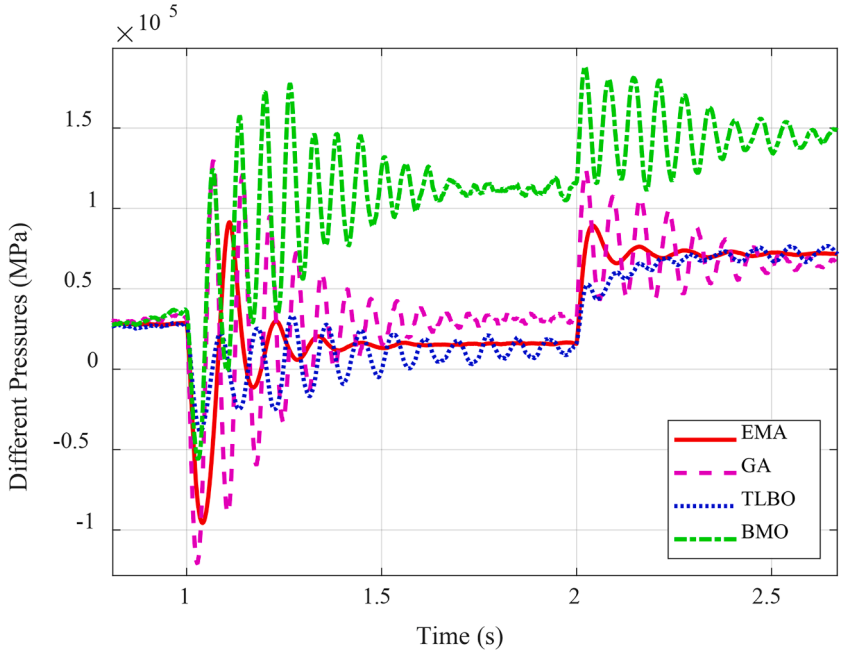

Fig. 9. Sample of different pressures in cylinder between AD-PPC-PID with EMA vs. AD-PPC-PID with other optimzers for multi-step input trajectory.

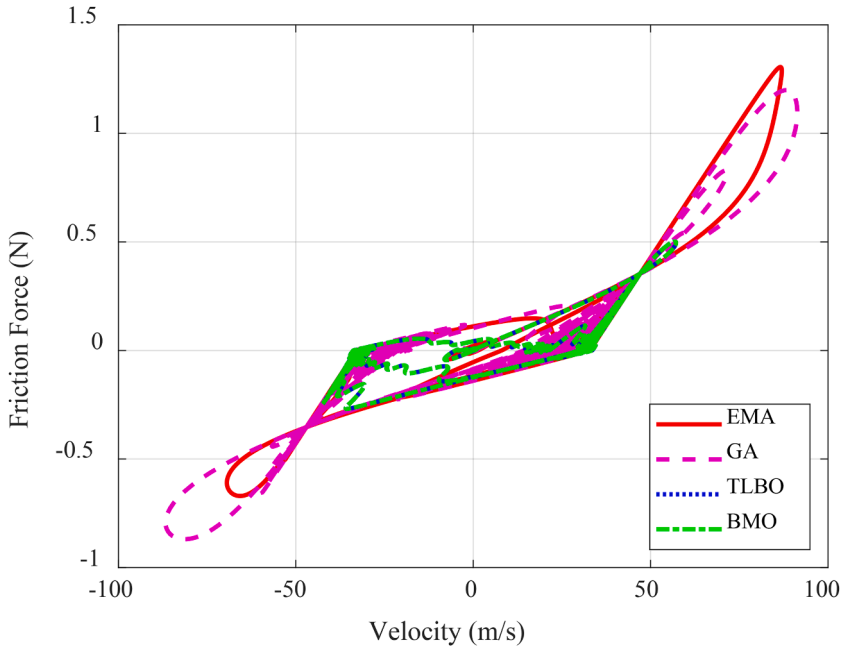

Fig. 10. Sample of friction force versus velocity curve performances for multi-steps input trajectory.

influence the work reported in this paper.

Data availability

The data that has been used is confidential.

Acknowledgement

The authors would like to thank the Ministry of Higher Education for providing financial support under Fundamental research grant No. FRGS/1/2019/TK04/UMP/02/1 (University reference RDU1901106) and Universiti Malaysia Pahang for laboratory facilities.

References

[1] Qian P, Pu C, Liu L, He D, Ruiz Páez LM, Meng D. A novel high-frequency resonance controllable pneumatic actuator and its high-precision motion trajectory tracking control. Mechatronics 2023;96:103089. https://doi.org/10.1016/j.mechatronics.2023.103089. 2023/12/01/.
[2] Wit CCd, Olsson H, Astrom KJ, Lischinsky P. A new model for control of systems with friction. IEEE Trans Automat Contr 1995;40(3):419–25. https://doi.org/10.1109/9.376053.
[3] J.A. Riofrío, C. Woodrow, and J. Mallory, "Modeling, simulation and experimental validation of a servo-pneumatic control system with off-the-shelf components," no. 57236, p. V001T01A012, 2015, doi: 10.1115/FPMC2015-9519.
[4] Endler L, De Negri VJ, Castelan EB. Compressed air saving in symmetrical and asymmetrical pneumatic positioning systems. Proc Inst Mech Eng, Part I: J Syst Control Eng 2015;229(10):957–69. https://doi.org/10.1177/0959651815597819. 2015/11/01.
[5] Liu Z, Yin X, Peng K, Wang X, Chen Q. Soft pneumatic actuators adapted in multiple environments: a novel fuzzy cascade strategy for the dynamics control with hysteresis compensation. Mechatronics 2022;84:102797. https://doi.org/10.1016/j.mechatronics.2022.102797. 2022/06/01/.
[6] Zhang R, Xu Z, Yang Y, Zhu P. Uncertainty-Estimation-Based Prescribed Performance Pressure Control for Train Electropneumatic Brake Systems. Actuators 2023;12(10):372 [Online]. Available: https://www.mdpi.com/2076-0825/12/10/372.
[7] Xiao H, Meng Q, Lai X, Yan Z, Zhao S, Wu M. Inverse Compensation Feedforward Control Strategy for a Vertical Pneumatic Artificial Muscle System. In: 2022 8th International Conference on Control Science and Systems Engineering (ICCSSE); 2022. p. 35–9. https://doi.org/10.1109/ICCSSE55346.2022.10079857. 14-16 July 2022.
[8] Chan CY, Chong SH, Loh SL, Alias A, Kasdirin HA. Positioning Control of an Antagonistic Pneumatic Muscle Actuated System using Feedforward Compensation with Cascaded Control Scheme. International Journal of Integrated Engineering 2020;12(2):70–4. 02/28[Online]. Available: https://publisher.uthm.edu.my/ojs/index.php/ijie/article/view/5301.
[9] I.S. Trenev and D.D. Devyatkin, "Feedback Linearization Control of Nonlinear System," *Eng Proc*, vol. 33, no. 1, doi: 10.3390/engproc2023033036.
[10] Huang H, Lin J, Wu L, Fang B, Sun F. Optimal control scheme for pneumatic soft actuator under comparison of proportional and PWM-solenoid valves. Photonic Network Communications 2019;37(2):153–63. https://doi.org/10.1007/s11107-018-0815-3. 2019/04/01.
[11] D. Hu, G. Li, and F. Deng, "Gain-Scheduled Model Predictive Control for a Commercial Vehicle Air Brake System," *Processes*, vol. 9, no. 5, doi: 10.3390/pr9050899.
[12] Zhang R, et al. A predictive control method to improve pressure tracking precision and reduce valve switching for pneumatic brake systems. IET Control Theory & Applications 2021;15(10):1389–403. https://doi.org/10.1049/cth2.12130. 2021/07/01.
[13] Silva F, Duarte M, Correia L, Oliveira SM, Christensen AL. Open Issues in Evolutionary Robotics. Evol Comput 2016;24(2):205–36. https://doi.org/10.1162/EVCO_a_00172.
[14] Azahar MIP, Irawan A, Raja Ismail RMT. Adjustable Convergence Rate Prescribed Performance with Fractional-Order PID Controller for Servo Pneumatic Actuated Robot Positioning. Cognitive Robotics 2023;3:93–106. https://doi.org/10.1016/j.cogr.2023.04.004. Article.
[15] Zhang Z, Jin Z, Gu GX. Efficient pneumatic actuation modeling using hybrid physics-based and data-driven framework. Cell Reports Physical Science 2022;3(4):100842. https://doi.org/10.1016/j.xcrp.2022.100842. 2022/04/20/.
[16] Momeni Z, Bagchi A. Multi-objective control optimization of isolated bridge using replicator controller and NSGA-II. Heliyon 2023;9(9):e19381. https://doi.org/10.1016/j.heliyon.2023.e19381. 2023/09/01/.
[17] Maayah B, Arqub OA. Uncertain M-fractional differential problems: existence, uniqueness, and approximations using Hilbert reproducing technique provisioner with the case application: series resistor-inductor circuit. Phys Scr 2024;99(2):025220. https://doi.org/10.1088/1402-4896/ad1738. 2024/01/09.
[18] Abu Arqub O, Mezghiche R, Maayah B. Fuzzy M-fractional integrodifferential models: theoretical existence and uniqueness results, and approximate solutions utilizing the Hilbert reproducing kernel algorithm," (in English). Front Phys 2023;11. https://doi.org/10.3389/fphy.2023.1252919. Original Research2023-October-02.
[19] Abu Arqub O. Numerical solutions for the Robin time-fractional partial differential equations of heat and fluid flows based on the reproducing kernel algorithm. Int J Numer Methods Heat Fluid Flow 2018;28(4):828–56. https://doi.org/10.1108/HFF-07-2016-0278.
[20] Wen N, Liu Z, Wang W, Wang S. Feedback linearization control for uncertain nonlinear systems via generative adversarial networks. ISA Trans 2023. https://doi.org/10.1016/j.isatra.2023.12.033. 2023/12/29/.
[21] Yang L, Wang R, Ding R, Liu W, Zhu Z. Investigation on the dynamic performance of a new semi-active hydro-pneumatic inerter-based suspension system with MPC control strategy. Mech Syst Signal Process 2021;154:107569. https://doi.org/10.1016/j.ymssp.2020.107569. 2021/06/01/.
[22] K. Lu, G. Feng, and B. Ding, "Robust H-Infinity Tracking Control for a Valve-Controlled Hydraulic Motor System with Uncertain Parameters in the Complex Load Environment," *Sensors*, vol. 23, no. 22, doi: 10.3390/s23229092.
[23] Liu J, et al. μ-Synthesis control with reference model for aeropropulsion system test facility under dynamic coupling and uncertainty. Chinese Journal of Aeronautics 2023;36(10):246–61. https://doi.org/10.1016/j.cja.2023.06.016. 2023/10/01/.
[24] Sun H, Gao L, Zhao Z, Li B. Adaptive super-twisting fast nonsingular terminal sliding mode control with ESO for high-pressure electro-pneumatic servo valve. Control Eng Pract 2023;134:105483. https://doi.org/10.1016/j.conengprac.2023.105483. 2023/05/01/.
[25] Adam NM, Irawan A, Ahmad MA. Robust super-twisting sliding mode controller for the lateral and longitudinal dynamics of rack steering vehicle. Bulletin of Electrical Engineering and Informatics 2022;11(4):1882–91. https://doi.org/10.11591/eei.v11i4.3641. Article.
[26] Aschemann H, Prabel R, Schindele D. Hysteresis compensation and adaptive LQR design for an electro-pneumatic clutch for heavy trucks. In: 2013 European Control Conference (ECC); 2013. p. 1475–80. https://doi.org/10.23919/ECC.2013.6669622. 17-19 July 2013.
[27] Wang J, Shao C, Chen Y-Q. Fractional order sliding mode control via disturbance observer for a class of fractional order systems with mismatched disturbance. Mechatronics 2018;53:8–19. https://doi.org/10.1016/j.mechatronics.2018.05.006. 2018/08/01/.
[28] J. Rwafa and F. Ghayoor, "Implementation of Iterative Learning Control on a Pneumatic Actuator," *Actuators*, vol. 11, no. 8, doi: 10.3390/act11080240.
[29] Sun Y, Zhang Y, Qin H, Ouyang L, Jing R. Predefined-time prescribed performance control for AUV with improved performance function and error transformation. Ocean Engineering 2023;281:114817. https://doi.org/10.1016/j.oceaneng.2023.114817. 2023/08/01/.
[30] Ueno K, Kawamura S, Deng M. Operator-Based Nonlinear Control for a Miniature Flexible Actuator Using the Funnel Control Method. Machines 2021;9(2):26 [Online]. Available: https://www.mdpi.com/2075-1702/9/2/26.
[31] Ai Q, et al. High-Order Model-Free Adaptive Iterative Learning Control of Pneumatic Artificial Muscle With Enhanced Convergence. IEEE Transactions on Industrial Electronics 2020;67(11):9548–59. https://doi.org/10.1109/TIE.2019.2952810.
[32] Qian K, Li Z, Chakrabarty S, Zhang Z-L, Xie S. Robust Iterative Learning Control for Pneumatic Muscle With Uncertainties and State Constraints. IEEE Transactions on Industrial Electronics 2023;70:1802–10.
[33] Ilchmann A, Ryan EP, Trenn S. Tracking control: performance funnels and prescribed transient behaviour. Syst Control Lett 2005;54(7):655–70. https://doi.org/10.1016/j.sysconle.2004.11.005. 2005/07/01/.
[34] Bechlioulis CP, Rovithakis GA. Robust Adaptive Control of Feedback Linearizable MIMO Nonlinear Systems With Prescribed Performance. IEEE Trans Automat Contr 2008;53(9):2090–9. https://doi.org/10.1109/TAC.2008.929402.

[35] Hackl CM, Endisch C, Schroder D. Funnel-Control in robotics: an introduction. In: 2008 16th Mediterranean Conference on Control and Automation; 2008. p. 913–9. https://doi.org/10.1109/MED.2008.4602041. 25-27 June 2008.

[36] Zhang C, Na J, Wu J, Chen Q, Huang Y. Proportional-Integral Approximation-Free Control of Robotic Systems with Unknown Dynamics. IEEE/ASME Transactions on Mechatronics 2020. https://doi.org/10.1109/TMECH.2020.3035660. 1-1.

[37] Na J, Huang Y, Wu X, Gao G, Herrmann G, Jiang JZ. Active Adaptive Estimation and Control for Vehicle Suspensions With Prescribed Performance. IEEE Transactions on Control Systems Technology 2018;26(6):2063–77. https://doi.org/10.1109/TCST.2017.2746060.

[38] K. Ueno, S. Kawamura, and M. Deng, "Operator-Based Nonlinear Control for a Miniature Flexible Actuator Using the Funnel Control Method," *Machines*, vol. 9, no. 2, doi: 10.3390/machines9020026.

[39] Poursadegh A, Shahnazi R, Yin S. Funnel-based adaptive fuzzy finite-time control for non-affine nonlinear systems preceded by unknown actuators. J Franklin Inst 2022;359(17):9591–617. https://doi.org/10.1016/j.jfranklin.2022.09.061. 2022/11/01/.

[40] Liu YH, Su CY, Li H. Adaptive Output Feedback Funnel Control of Uncertain Nonlinear Systems With Arbitrary Relative Degree. IEEE Trans Automat Contr 2021; 66(6):2854–60. https://doi.org/10.1109/TAC.2020.3012027.

[41] Verginis CK. Funnel Control for Uncertain Nonlinear Systems via Zeroing Control Barrier Functions. IEEE Control Syst Lett 2023;7:853–8. https://doi.org/10.1109/LCSYS.2022.3227514.

[42] Du H, Yuan T, Xiong W. Cylinder position control driven by pneumatic digital bridge circuit using a fuzzy algorithm under large stroke and varying load conditions. J Franklin Inst 2023;360(8):5892–909. https://doi.org/10.1016/j.jfranklin.2023.04.007. 2023/05/01/.

[43] Azahar MIP, Irawan A, Taufika R. Fuzzy Self-Adaptive Sliding Mode Control for Pneumatic Cylinder Rod-Piston Motion Precision Control. Journal of Physics: Conference Series 2020;1532:012028. https://doi.org/10.1088/1742-6596/1532/1/012028. 06/01.

[44] Karahan M, Lacinkaya F, Erdonmez K, Eminagaoglu ED, Kasnakoglu C. Age and gender classification from facial features and object detection with machine learning. Journal of Fuzzy Extension and Applications 2022;3(3):219–30. https://doi.org/10.22105/jfea.2022.328472.1201.

[45] Chen Y, Tao G, Meng F. An Intelligent Adaptive Robust Controller Based on Neural Network for a Pneumatic System. IOP Conference Series: Materials Science and Engineering 2019;575(1):012016. https://doi.org/10.1088/1757-899X/575/1/012016. 2019/07/01.

[46] Chaturvedi S, Kumar N, Kumar R. Two Feedback PID Controllers Tuned with Teaching–Learning-Based Optimization Algorithm for Ball and Beam System. IETE J Res 2023:1–10. https://doi.org/10.1080/03772063.2023.2284955.

[47] Al-Dhaifallah M, Kanagaraj N, Nisar KS. Fuzzy Fractional-Order PID Controller for Fractional Model of Pneumatic Pressure System. Math Probl Eng 2018;2018: 5478781. https://doi.org/10.1155/2018/5478781. 2018/02/28.

[48] Ren H, Fan J, Kaynak O. Optimal Design of a Fractional-Order Proportional-Integer-Differential Controller for a Pneumatic Position Servo System. IEEE Transactions on Industrial Electronics 2019;66(8):6220–9. https://doi.org/10.1109/TIE.2018.2870412.

[49] Wang N, Wang Y. Fuzzy Adaptive Quantized Tracking Control of Switched High-Order Nonlinear Systems: a New Fixed-Time Prescribed Performance Method. IEEE Transactions on Circuits and Systems II: Express Briefs 2022;69(7):3279–83. https://doi.org/10.1109/TCSII.2022.3143996.

[50] Shao X, Hu Q, Shi Y, Jiang B. Fault-Tolerant Prescribed Performance Attitude Tracking Control for Spacecraft Under Input Saturation. IEEE Transactions on Control Systems Technology 2020;28(2):574–82. https://doi.org/10.1109/TCST.2018.2875426.

[51] Markom MA, Adom AH, Shukor SAA, Rahim NA, Tan ESMM, Irawan A. Scan matching and KNN classification for mobile robot localisation algorithm. In: 2017 IEEE 3rd International Symposium in Robotics and Manufacturing Automation, ROMA 2017. 2017-December; 2017. p. 1–6. https://doi.org/10.1109/ROMA.2017.8231836.

[52] Soh SC, Ibrahim MZ, Abas MF, Sulaiman N, Mulvaney DJ. Image Fusion based Multi Resolution and Frequency Partition Discrete Cosine Transform for Palm Vein Recognition. In: 2019 IEEE 6th International Conference on Industrial Engineering and Applications (ICIEA); 2019. p. 367–71. https://doi.org/10.1109/IEA.2019.8715136. 12-15 April 2019.

[53] Tan WK, Ismail MAH, Husin Z, Yasruddin ML. Automated Tomato Grading System using Computer Vision (CV) and Deep Neural Network (DNN) Algorithm. In: 2022 IEEE 12th Symposium on Computer Applications & Industrial Electronics (ISCAIE); 2022. p. 22–7. https://doi.org/10.1109/ISCAIE54458.2022.9794557. 21-22 May 2022.

[54] Dhami SS. A Hybrid Controller for Position Control of a Pneumatic Actuator under Variable Loading Conditions. MATEC Web Conf 2017;95. https://doi.org/10.1051/matecconf/20179516001 [Online]. Available:.

[55] Azahar MIP, Irawan A, Ismail RMTR. Self-tuning hybrid fuzzy sliding surface control for pneumatic servo system positioning. Control Eng Pract 2021;113: 104838. https://doi.org/10.1016/j.conengprac.2021.104838. 2021/08/01/.

[56] Wang C, Shi Y, Wang Y, Xu S, Sun Z. Position Tracking Control for Pneumatic Servo System Subject to State Constraints and Voltage Saturation. IEEE/ASME Transactions on Mechatronics 2023:1–11. https://doi.org/10.1109/TMECH.2023.3336281.

[57] Y. Dai, Z. Deng, X. Wang, and H. Yuan, "A Hybrid Controller for a Soft Pneumatic Manipulator Based on Model Predictive Control and Iterative Learning Control," *Sensors*, vol. 23, no. 3, doi: 10.3390/s23031272.

[58] Haupt RL, Haupt SE. Practical genetic algorithms. 2nd ed. John Wiley & Sons; 2004.

[59] Edalatpanah SA, Hassani FS, Smarandache F, Sorourkhah A, Pamucar D, Cui B. A hybrid time series forecasting method based on neutrosophic logic with applications in financial issues. Eng Appl Artif Intell 2024;129:107531. https://doi.org/10.1016/j.engappai.2023.107531. 2024/03/01/.

[60] Dirik M. Detection of counterfeit banknotes using genetic fuzzy system (in en) Journal of Fuzzy Extension and Applications 2022;3(4):302–12. https://doi.org/10.22105/jfea.2022.345344.1223.

[61] Arqub OA, Abo-Hammour Z. Numerical solution of systems of second-order boundary value problems using continuous genetic algorithm. Inf Sci (Ny) 2014; 279:396–415. https://doi.org/10.1016/j.ins.2014.03.128. 2014/09/20/.

[62] Costa Filho RND, Paucar VL. A multi-objective optimization model for robust tuning of wide-area PSSs for enhancement and control of power system angular stability. Results in Control and Optimization 2021;3:100011. https://doi.org/10.1016/j.rico.2021.100011. 2021/06/01/.

[63] Masuri A, Medina O, Hacohen S, Shvalb N. Gait and Trajectory Optimization by Self-Learning for Quadrupedal Robots with an Active Back Joint. Journal of Robotics 2020;2020:8051510. https://doi.org/10.1155/2020/8051510. 2020/06/10.

[64] Kureychick VM, Kaplunov TG. Time series forecasting method based on genetic algorithm for predicting the conditions of technical systems. Journal of Physics: Conference Series 2019;1333(3):032046. https://doi.org/10.1088/1742-6596/1333/3/032046. 2019/10/01.

[65] Al-Douri YK, Hamodi H, Lundberg J. Time Series Forecasting Using a Two-Level Multi-Objective Genetic Algorithm: a Case Study of Maintenance Cost Data for Tunnel Fans. Algorithms 2018;11(8):123 [Online]. Available: https://www.mdpi.com/1999-4893/11/8/123.

[66] Storn R, Price K. Differential Evolution – A Simple and Efficient Heuristic for global Optimization over Continuous Spaces. Journal of Global Optimization 1997; 11(4):341–59. https://doi.org/10.1023/A:1008202821328. 1997/12/01.

[67] Xin Y, Yong L, Guangming L. Evolutionary programming made faster. IEEE Transactions on Evolutionary Computation 1999;3(2):82–102. https://doi.org/10.1109/4235.771163.

[68] Eberhart R, Kennedy J. A new optimizer using particle swarm theory. In: MHS'95. Proceedings of the Sixth International Symposium on Micro Machine and Human Science; 1995. p. 39–43. https://doi.org/10.1109/MHS.1995.494215. 4-6 Oct. 1995.

[69] Yang H, Qi J, Miao Y, Sun H, Li J. A New Robot Navigation Algorithm Based on a Double-Layer Ant Algorithm and Trajectory Optimization. IEEE Transactions on Industrial Electronics 2019;66(11):8557–66. https://doi.org/10.1109/TIE.2018.2886798.

[70] Irawan A, Ramli MS, Sulaiman MH, Azahar MIP, Adom AH. Optimal Pneumatic Actuator Positioning and Dynamic Stability using Prescribed Performance Control with Particle Swarm Optimization: a Simulation Study. International Journal of Robotics and Control Systems 2023;3(3):16. https://doi.org/10.31763/ijrcs.v3i3.1002. 2023-05-29.

[71] Zulkifli NN, Ramli MS, Ahmad H, Irawan A. FRIT-based integral action state feedback controller tuning using PSO for a liquid slosh suppression system. Bulletin of Electrical Engineering and Informatics 2022;11(3):1260–71. https://doi.org/10.11591/eei.v11i3.3262. Article.

[72] Dirik M. Type-2 fuzzy logic controller design optimization using the PSO approach for ECG prediction (in en) Journal of Fuzzy Extension and Applications 2022; 3(2):158–68. https://doi.org/10.22105/jfea.2022.333786.1207.

[73] Karaboga D, Basturk B. On the performance of artificial bee colony (ABC) algorithm. Appl Soft Comput 2008;8(1):687–97. https://doi.org/10.1016/j.asoc.2007.05.007. 2008/01/01/.
[74] Mirjalili S, Mirjalili SM, Lewis A. Grey Wolf Optimizer. Advances in Engineering Software 2014;69:46–61. https://doi.org/10.1016/j.advengsoft.2013.12.007. 3//.
[75] Shahabi F, Poorahangaryan F, Edalatpanah SA, Beheshti H. A Multilevel Image Thresholding Approach Based on Crow Search Algorithm and Otsu Method. Int J Comput Intell Appl 2020;19(02):2050015. https://doi.org/10.1142/S1469026820500157. 2020/06/01.
[76] Sulaiman MH, Mustaffa Z, Saari MM, Daniyal H. Barnacles Mating Optimizer: a new bio-inspired algorithm for solving engineering optimization problems. Eng Appl Artif Intell 2020;87:103330. https://doi.org/10.1016/j.engappai.2019.103330. 2020/01/01/.
[77] Rashedi E, Nezamabadi-pour H, Saryazdi S. GSA: a Gravitational Search Algorithm. Inf Sci (Ny) 2009;179(13):2232–48. https://doi.org/10.1016/j.ins.2009.03.004. 2009/06/13/.
[78] Lee KS, Geem ZW. A new meta-heuristic algorithm for continuous engineering optimization: harmony search theory and practice. Comput Methods Appl Mech Eng 2005;194(36):3902–33. https://doi.org/10.1016/j.cma.2004.09.007. 2005/09/23/.
[79] Tuvayanond W, Parnichkun M. Position control of a pneumatic surgical robot using PSO based 2-DOF H∞ loop shaping structured controller. Mechatronics 2017;43:40–55. https://doi.org/10.1016/j.mechatronics.2017.03.001. 2017/05/01/.
[80] Ayinla SL, et al. Optimal control of DC motor using leader-based Harris Hawks optimization algorithm. Franklin Open 2024;6:100058. https://doi.org/10.1016/j.fraope.2023.100058. 2024/03/01/.
[81] Wang S, Jin X. Model-based optimal control of VAV air-conditioning system using genetic algorithm. Build Environ 2000;35(6):471–87. https://doi.org/10.1016/S0360-1323(99)00032-3. 2000/08/01/.
[82] Bandong S, Kirana RC, Nazaruddin YY, Joelianto E. Optimal Gantry Crane PID Controller Based on LQR With Prescribed Degree of Stability by Means of GA, PSO, and SA. In: 2022 7th International Conference on Electric Vehicular Technology (ICEVT); 2022. p. 46–51. https://doi.org/10.1109/ICEVT55516.2022.9925018. 14-16 Sept. 2022.
[83] B. Grüter, J. Diepolder, M. Bittner, F. Holzapfel, and J.Z. Ben-Asher, "Bi-level Cross Entropy Method and Optimal Control for Air Traffic Sequencing and Trajectory Optimization," in *AIAA Scitech 2020 Forum*.
[84] Sulaiman MH, Mustaffa Z, Saari MM, Daniyal H, Mirjalili S. Evolutionary mating algorithm. Neural Computing and Applications 2023;35(1):487–516. https://doi.org/10.1007/s00521-022-07761-w. 2023/01/01.
[85] Irawan A, Azahar MIP, Hashimi MA. Sensorless force estimation on fingertip with gravitational compensation for heavy-duty pneumatic tri-grasper robot. In: IET Conference Proceedings. Institution of Engineering and Technology; 2022. p. 1–5.
[86] Irawan A, Azahar MIP. Cascade Control Strategy on Servo Pneumatic System with Fuzzy Self-Adaptive System. Journal of Control, Automation and Electrical Systems 2020;31(6):1412–25. https://doi.org/10.1007/s40313-020-00642-4. 2020/12/01.
[87] Irawan A, Azahar MIP, Pebrianti D. Interaction Motion Control on Tri-finger Pneumatic Grasper using Variable Convergence Rate Prescribed Performance Impedance Control with Pressure-based Force Estimator. Journal of Robotics and Control (JRC) 2022;3(5):9. https://doi.org/10.18196/jrc.v3i5.16316. 2022-09-01.
[88] Azahar MIP, Irawan A, Ramli MS. Finite-Time Prescribed Performance Control for Dynamic Positioning of Pneumatic Servo System. In: 2020 IEEE 8th Conference on Systems, Process and Control (ICSPC); 2020. p. 1–6. https://doi.org/10.1109/ICSPC50992.2020.9305755. 11-12 Dec. 2020.
[89] Suseno E, Ma'arif A. Tuning of PID Controller Parameters with Genetic Algorithm Method on DC Motor. International Journal of Robotics and Control Systems 2021;1:41–53. https://doi.org/10.31763/ijrcs.v1i1.249. 02/22.
[90] Rao RV. Teaching learning based optimization algorithm: and its engineering applications. Springer Publishing Company; 2015. Incorporated.
[91] Azahar MIP, Irawan A, Taufika RM, Suid MH. Position Control of Pneumatic Actuator Using Cascade Fuzzy Self-adaptive PID. In: Singapore, 2020: Springer Singapore, in InECCE; 2019. p. 3–14.
[92] Irawan A, Azahar MIP, Ismail ZH. Interaction Motion on Pneumatic Cylinder using Prescribed Performance Force Tracking Impedance Control. In: 2020 8th International Conference on Control, Mechatronics and Automation, ICCMA 2020; 2020. p. 121–6. https://doi.org/10.1109/ICCMA51325.2020.9301501.
[93] Azahar MIP, Irawan A, Taufika RM. Fuzzy Self-Adaptive PID for Pneumatic Piston Rod Motion Control. In: ICSGRC 2019 - 2019 IEEE 10th Control and System Graduate Research Colloquium, Proceeding; 2019. p. 82–7. https://doi.org/10.1109/ICSGRC.2019.8837064.
[94] Wojewoda J, Stefański A, Wiercigroch M, Kapitaniak T. Hysteretic effects of dry friction: modelling and experimental studies. Philosophical Transactions of the Royal Society A: Mathematical, Physical and Engineering Sciences 2008;366(1866):747–65. https://doi.org/10.1098/rsta.2007.2125.